

Control of Charge Dilution in Turbocharged Diesel Engines via Exhaust Valve Timing

Hakan Yilmaz and Anna Stefanopoulou
University of Michigan, Ann Arbor

Abstract

Stringent constraints in oxides of nitrogen (NO_x) and particulate emission require high levels of exhaust gas recirculation. In this paper we employ a Variable Valve Timing methodology that in steady-state achieves large levels of internal Exhaust Gas Recirculation (iEGR) or charge dilution in Diesel engines. We develop a crankangle based dynamic nonlinear model of a six-cylinder 12 liter turbocharged (TC) Diesel engine. This model captures the transient interactions between VVT actuation, the turbocharger dynamics, and the cylinder-to-cylinder breathing characteristics. Low order linear multi-input multi-output (MIMO) models are then identified using cycle-sampled or -averaged data from the higher order nonlinear model. A model-based controller is designed that varies Exhaust Valve Closing (EVC) to maximize the internal exhaust gas recirculation under air-to-fuel ratio (AFR) constraints during transient fueling demands. The closed-loop controller is based on tracking optimal and achievable set-points of burned gas fraction. Simulation results are shown on the full order model.

1. Introduction

Diesel or Compression Ignition Direct Injection (CIDI) engine manufacturers use exhaust gas recirculation (EGR) to reduce the peak cylinder temperature [3, 4], and consequently, reduce oxides of nitrogen (NO_x) emissions. With proper control, reduced NO_x levels can be achieved without significant power and particulate emissions penalties. Moreover, in Homogeneous Charge Compression Ignition (HCCI) engines high level of EGR can be used to indirectly control combustion initiation. Consequently, achieving fast and accurate control of EGR is an important objective for conventional diesel and HCCI engines [7, 10].

Conventional external EGR (eEGR), relies on a pressure drop from exhaust manifold to intake manifold. The flow of eEGR is typically regulated by the EGR valve. Well-tuned and highly efficient CIDI engines often operate under conditions where intake manifold pressure is higher than the exhaust manifold pressure. Such engines require additional hardware for achieving external EGR, such as a venturi system, intake EGR throttle, Variable Geometry Turbocharger (VGT), or exhaust back-pressure valve (see Figure 1). All these mechanisms, have either limited range of operation, or achieve the required EGR level by

throttling the intake or exhaust flow, and therefore, reducing the efficiency of turbocharged CIDI engines. Moreover, these mechanisms do not allow fast control of in-cylinder AFR excursions during fueling transients because cylinder charge is controlled indirectly through the turbocharger and the intake manifold [3, 9]. The system dynamics is, thus, limited by the intake and exhaust manifold filling and turbocharger dynamics.

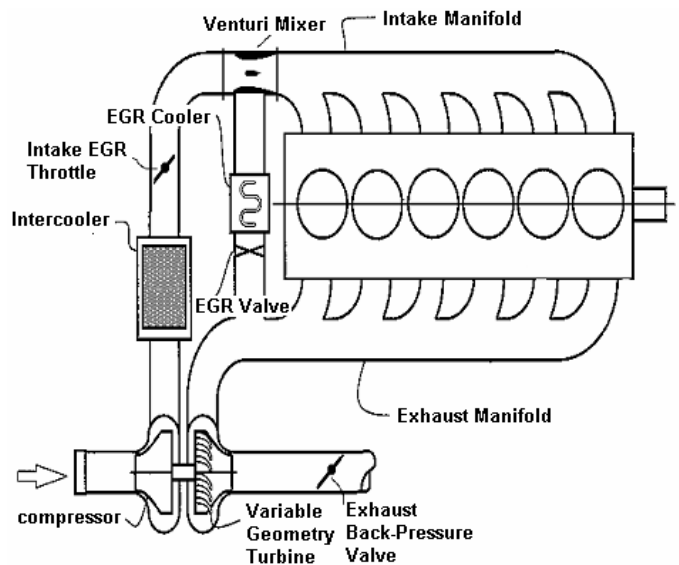


Figure 1. Current External EGR Applications : Venturi Mixer, Intake EGR Throttle, Variable Geometry Turbocharger, Exhaust Back-Pressure Valve

Internal Exhaust Gas Recirculation (iEGR), is an alternative method for achieving EGR, can avoid losses that are associated with pumping exhaust gas from the exhaust manifold to the intake manifold through an eEGR valve [8]. By employing Variable Valve Timing (VVT), an iEGR approach can achieve to the dilution level by Early Exhaust Valve Closing (eEVC), Late Exhaust Valve Closing (lEVC) or re-opening on the induction stroke [2]. In this work, due to piston geometry limitations, eEVC is selected as the VVT degree of freedom to achieve EGR control.

Using a crank angle based, non-linear, dynamic model of a direct-injection, turbocharged diesel engine [6], we examine the potential of VVT-regulated iEGR for future engine applications. Transient and steady-state response of the engine with VVT is analyzed using the high order non-

linear model, and these results are used to create lower order linear models and feedforward control laws. Feedback controllers are then designed to regulate *EGR* subject to *AFR* performance constraints.

2. Crank Angle Based Model

In a multi-cylinder application, VVT will produce effects that depend on interactions between the various cylinders and the manifolds that connect them. We employ the standard spatially averaged, zero-dimensional model similar to [5, 11]. We, thus, develop a non-linear a non-linear crank angle-based dynamic model of mass and heat flows in which cylinder volumes are considered individually and intake and exhaust manifolds are lumped into volumes that are coupled to the cylinders and to each other. Each component includes three state variables representing the mass, the pressure, and the burned gas fraction of the respective component. The differential equations for the state variables are derived from the ideal gas law, conservation of energy, conservation of mass, and an assumption that each component is a plenum with homogeneous temperature, pressure and density. The torque (Tq) produced at the crankshaft is calculated based on the individual cylinder pressure and piston motion using the idealized slider-crank mechanism. The resulting model has 29 crank-angle resolved states. We augment the model with additional states that correspond to the integrators for the cycle averaged variables. This model has been initially developed for control of compression braking (secondary exhaust valve opening during the compression stroke) in [6]. The model has been augmented with exhaust valve closing variability and states for burned gas fraction.

3. Variable Valve Timing Approach

Figure 2 shows simulation results with three values of *EVC* timing resulting in three different values for *iEGR*. The direction of the arrows indicates the progression of intake and exhaust flows over the range of changing *EVC*. The first curve in each progression (as indicated by the direction of each arrow) corresponds to the original exhaust valve profile, with *EVC* at 404 degrees after TDC. *EVC* is then advanced about 25 degrees and then 50 degrees. Early *EVC* closing increases the exhaust gas trapped in the cylinder and causes re-compression at the end of the exhaust stroke. The resulting high in-cylinder pressure causes some amount of residual gas to flow into the intake manifold. When the cylinder pressure value drops below the intake manifold pressure value, induction begins, starting with the recently expelled residuals, thereby augmenting *iEGR* that can be regulated with a single actuator, namely the *EVC*.

3.1 Cycle-Sampled or Averaged Behavior

High order nonlinear crankangle-based dynamical model enhances our understanding and is used to model the cycle-resolved input-output system behavior. The controlled

variable, *EVC*, is a cycle-resolved variable and thus a cycle-averaged model-based controller is required. The performance variables of interest are torque (Tq), *AFR*, and burned gas fraction (F_{cyl}). Conventional production sensors provide the intake manifold pressure (p_i).

We create a series of linear, time averaged, models, by processing the crankangle-resolved data to obtain the input-output cycle-sampled behavior. The output data from the simulation is recorded every 2 crank angle degrees. The cycle-averaged intake manifold pressure and torque are obtained as arithmetic averages of the crankangle resolved data. This arithmetic average value is assigned to the whole cycle period. The in-cylinder burned gas fraction (F_{cyl}) is sampled for every cylinder and every cycle just before the combustion initiation. The value of the burned gas fraction before combustion corresponds to the charge dilution which affects the combustion characteristics, and thus, the generated emissions. In-cylinder *AFR* cycle-resolved sampling is similarly performed; the sampling scheme captures the *AFR* just before the combustion starts and uses this as the relevant value until the next cycle combustion.

Simulation results for different speeds and loads show a consistent correlation between advanced *EVC* and increased burned gas fraction. It is possible to increase the burned gas fraction in the cylinder up to 14 %. This increase in the burned gas fraction is followed by relatively low degradation of *AFR* and mean torque. For extreme values of advanced *EVC* (50°) during medium speed - medium load conditions, *AFR* drops below the acceptable limits for visible smoke. During these operating conditions, effective *iEGR* can be achieved with lower value of advanced *EVC*, typically around $35^\circ - 40^\circ$. A degradation in the mean torque is observed as a result of the re-compression. However, even for excessively advanced *EVC* conditions (about 50°) the mean torque loss is around 5-9 % whereas the in-cylinder burned gas fraction is increased up to 14-18%. This loss in terms of torque might be tolerable for most operating conditions.

The inlet manifold pressure also decreases for advanced *EVC*. This occurs because the exhaust mass trapped in the cylinder reduces the energy transmitted from the exhaust gas to the turbine, and thus, reduces the *TC* speed. Consequently, this drop in the boost pressure amplifies the effects of the re-compression and compounds to a lower torque output as can be seen in the steady state mean torque maps (not included here due to space limitations). Using these steady-state maps, look up tables for the engine management system can be prepared in order to adjust the engine controller outputs, fueling rate, and *EVC* timing according to the inputs, pedal position, and engine speed. The feedforward based on look-up tables is augmented by a feedback controller designed in the following sections to improve the transient response and to robustify the closed loop system.

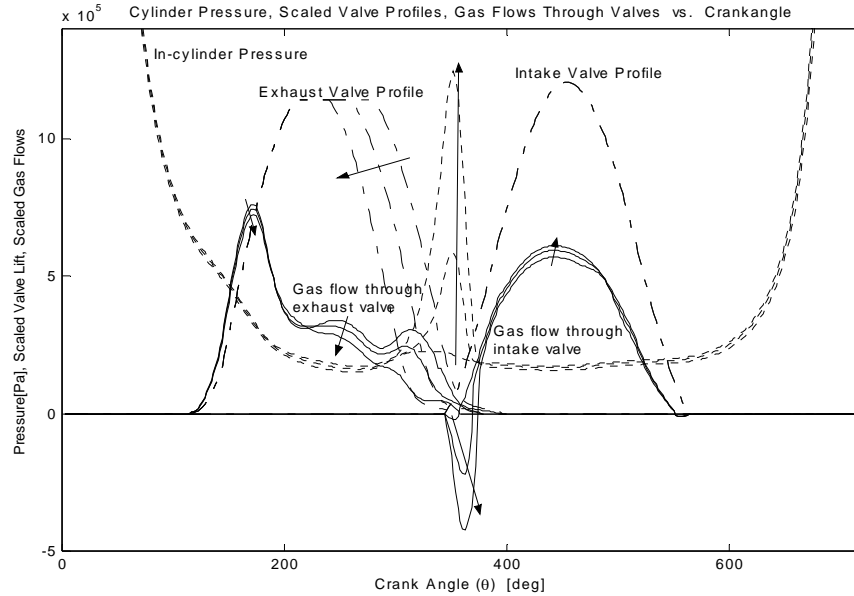


Figure 2 Quasi-static In-Cylinder Pressure, Valve Profiles, and Gas Flows Through Valves (scaled) vs. Crank Angle ($^{\circ}$)

Table 1 Optimal Set Points

Fuel Rate:	Optimum Exhaust Valve Closing Time (EVC)	Optimum Inlet Manifold Pressure (p_i)	Compressor Mass Flow rate (W_c)	% Torque Loss Compared to Zero EGR	Burned Gas Fraction in Cylinder (F_{cyl})
82 lb/hr	390°	199 kPa	304 g/sec	9 %	14 %
67 lb/hr	365°	168 kPa	238 g/sec	6 %	9 %
57 lb/hr	350°	148 kPa	197 g/sec	2 %	3 %

3.2 Identification of Linear Input/Output Model

In order to design a cycle-based feedback controller we perform multivariable linear system identification around a series of operating points corresponding to various torque and speed combinations. To select the operating points we first identify the fuel level that satisfies the torque demand for each speed, and then select from operating points corresponding to that fueling level the EVC which maximizes the burned gas fraction under AFR constraints [5]. For 1600 rpm engine speed, the optimal set points are shown in Table. The input/output behavior includes all the system inputs, namely, W_f as the disturbance and EVC as the control variable. The identification also includes all the system outputs, namely, $z=[Tq, AFR]$ as the performance variables, $y=[p_i]$ as the measured outputs. Note here that we include the exhaust manifold pressure as a potential measured output to explore the performance improvements associated with this extra sensor. To identify the linear system, we use step changes in W_f and EVC and sample the cycle-resolved dynamic response. The cycle-resolved data is then imported into the Matlab System Identification Toolbox, and the multi input multi output linear system parameters are identified using state space parametric model estimation technique N4SID.

System Identification is performed around the operating points corresponding to 1600 rpm, 57 lb/hr with EVC set to the original value of 404 degrees ATDC and the two advanced values, 350 and 395 degrees. These points cover the dynamic range of the EVC as an actuator, thereby providing information necessary to evaluate the suitability of the actuator approach and design a controller that accounts for the engine dynamics. A third order system captures the dynamical behavior of all the operating points allowing controller gain scheduling. Note here that the identified system might not be valid for frequencies higher than 10 rad/sec that corresponds to the cycle sampling frequency at 1600 rpm. Before the control design we apply input/output scaling in order to avoid numerical problems and capture the physical range of actuator authority and output significance. The output scale is $T_z = \text{diag}([1/100, 1/7])$ the measurement scale is $T_y = 1/10000$ and the input scaling is $T_u = \text{diag}([1/0.003, 1/50])$. The state space representation of the scaled identified system is:

$$\dot{x} = \begin{bmatrix} -1.571 & 0.307 & 2.545 \\ 6.510 & -25.710 & -33.058 \\ 0.813 & 1.023 & -14.095 \end{bmatrix} x + \begin{bmatrix} -9.610 & -7.691 \\ 51.085 & -9.364 \\ 3.885 & 6.861 \end{bmatrix} \begin{bmatrix} W_f \\ EVC \end{bmatrix} \quad (1)$$

with performance variables $z' = [z_1 \ z_2]$

$$\begin{bmatrix} T_q \\ AFR \end{bmatrix} = \begin{bmatrix} -0.01 & 0.002 & -0.06 \\ 0.04 & -0.97 & -0.23 \end{bmatrix} x + \begin{bmatrix} 3.23 & 1.64 \\ -0.35 & 0.12 \end{bmatrix} \begin{bmatrix} W_f \\ EVC \end{bmatrix} \quad (2)$$

and measurements y

$$y = p_I = \begin{bmatrix} -0.47 & 0.002 & -0.12 \end{bmatrix} x + \begin{bmatrix} 0.099 & 0.014 \end{bmatrix} \begin{bmatrix} W_f \\ EVC \end{bmatrix} \quad (3)$$

In transfer function notation the plant Input/Output relation is defined as:

$$\begin{bmatrix} z_1 \\ z_2 \end{bmatrix} = \begin{bmatrix} G_{z11} & G_{z12} \\ G_{z21} & G_{z22} \end{bmatrix} \begin{bmatrix} u_1 \\ u_2 \end{bmatrix} \text{ and } y = \begin{bmatrix} G_{y1} & G_{y2} \end{bmatrix} \begin{bmatrix} u_1 \\ u_2 \end{bmatrix} \quad (4)$$

All the variables above are considered as perturbations from the nominal values.

4. Controller Design

The goal of the controller design is to achieve high burned gas fraction in the cylinder, while satisfying the driver's torque demand and the smoke-limited AFR range. The set-points derived in the previous section show that high F_{cyl} is achieved when EVC is controlled to maintain a constant $AFR=30$ for all fueling rates at 1600 rpm. At lower engine speed (eg. $N=1100$ rpm) the overall AFR level is low, thus, EVC can be controlled to maintain a low but feasible $AFR=20$. We assume here that engine speed varies slower than the engine variables in consideration. We, thus, focus at the control design during constant engine speed with the intent to gain schedule between controllers for various engine speeds. Torque is primarily controlled by the commanded fuel flow, W_f , although, EVC can now affect engine torque in a significant way. Similarly, EVC and W_f affect AFR resulting in a coupled two-input two-output (TITO) system.

4.1 Measured Performance Variables

We first design a feedback controller for EVC assuming we can measure accurately the performance variables T_q and AFR as shown in Figure 3. A fast closed loop W_f controller provides good T_q response. Based on the reduced order model the transfer function is

$$G_{z11} = \frac{s^2 + 40s + 399.1}{s^2 + 40s + 401.6} \cong 1 \quad (5)$$

Note that the open loop pole and zero conglomeration of G_{z11} occur close to the frequency where the cycle-averaged model breaks down. We choose a simple integral controller

$$C_{11} = \frac{2.00}{s} \quad (6)$$

It corresponds to a closed loop time constant of 0.5 sec. A controller, C_{canc} , that cancels completely the AFR excursions during fueling changes can be derived from

$$\begin{aligned} AFR &= G_{z21}W_f + G_{z22}EVC = 0 \Rightarrow \\ EVC &= -\underbrace{(G_{z22})^{-1}G_{z21}}_{C_{canc}} W_f \end{aligned} \quad (7)$$

We call this controller from now on as the ‘‘cancellation controller’’. Using, $C_{dec} = C_{canc}$ and $C_{22}=0$ in Figure 3 i.e., no feedback for the AFR loop, we get the response shown in the solid line in Figure 4. The AFR is always constant due to the exact cancellation of the fuel disturbance. The T_q response resembles a first order lag with 0.5 sec time constant. This time constant is selected after considering driveline shuffle dynamics. This controller gives us insight to the coupling and coordination between the two actuators for a perfect AFR regulation [8]. The fast closed loop W_f controller provides good T_q response. Note here that if fuel was commanded as a step change, the torque would have a large overshoot due to the fast EVC command towards retarded values. Regulation of torque with fuel is necessary at this point to avoid large T_q overshoot due to the EVC retarding. Since a T_q sensor is not readily available for vehicle applications, one has to implement the torque feedback based on an in-cylinder pressure measurement, such as Peak Pressure (PP), or IMEP. Although in-cylinder pressure measurements are not entirely out of the question, they are very expensive and sensitive, and thus an alternative approach is considered.

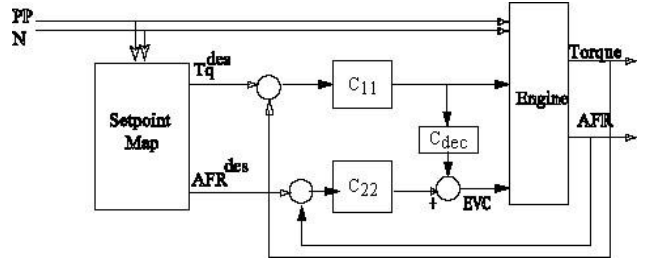


Figure 3. Block representation of AFR and T_q feedback

Advanced fuel injectors allow the use of open loop fuel commands based on look-up tables. We, thus, consider a filtered step change in W_f in response to a torque demand, instead of a closed loop W_f command. In other words, we can emulate the smooth fueling command of the closed loop $W_f - T_q$ by filtering an open loop fuel step. The controller architecture is shown in Figure 5. The fueling filter time constant is chosen to be 0.5 sec and

$$C_{filt} = \frac{1}{0.5s + 1} \quad (8)$$

Realizability based on EVC actuator constraints and the validity of the cycle-averaged model bandwidth are then considered. The cancellation controller is reduced to a static feedforward cross-coupling term from fuel to EVC

$$C_{dec} = C_{canc}(0) \quad (9)$$

by using the DC gain of the cancellation controller. $AFR-EVC$ feedback is then tuned as a lead-lag controller with an integrator. The static feedforward is an adequate level of coordination between the two inputs when the fast lead-lag from AFR to EVC is present. The static feedforward is actually necessary for small AFR excursions because it decouples the disturbance that W_f causes to AFR . Note here that the $EVC-AFR$ (lower) loop is designed to follow the $W_f - T_q$ response. Both loops are capable of achieving high bandwidth, but then the

interactions might be detrimental. We, thus, design the integrator plus lead-lag EVC - AFR controller

$$C_{22} = 2.73 \frac{(0.75s + 1)}{s(0.46s + 1)} \quad (10)$$

that results in a closed loop that cannot be fast enough to reject the W_f disturbance to AFR without a feedforward term. The linear feedback controller in Figure 5 with Equations (8), (9), and (10) shows good Tq and AFR response even during high charge dilution (see dashed line in Figure 4). The total burned gas fraction is $F_{cyl}=11\%$ at nominal fueling level and decreases down to $F_{cyl}=8\%$ in order to maintain $AFR=30$ during the increase in fueling level. In comparison, the conventional TC Diesel engine response is shown with the dotted line in Figure 4. The conventional engine operates at $F_{cyl}=1.5\%$ and $AFR=[30-42]$ with $EVC=404$.

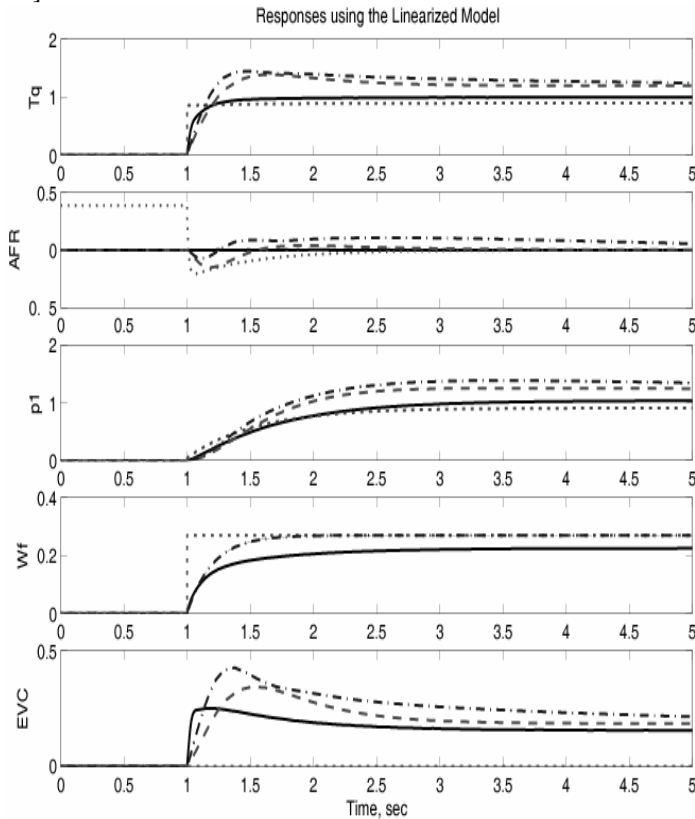


Figure 4. Linear system response

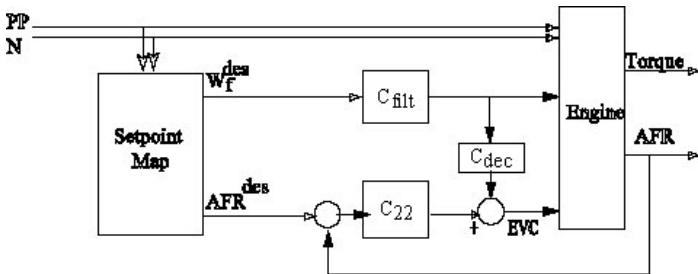


Figure 5. Block representation of AFR feedback and dynamic cancellation.

4.2 Measured Intake Manifold Pressure

We then analyze the closed loop performance limitations when conventional engine measurements, such as pressure (p_i) are used. It is important to note here that in the TC Diesel engine p_i is a measurement that correlates well with the engine pumping rate and thus AFR in the presence of variable EVC . An one-to-one steady-state coupling between p_i and AFR is maintained due to the turbocharger interaction between the intake and exhaust manifolds. Specifically, EVC affects AFR directly through the captured F_{cyl} , and indirectly through p_i (from EVC to p_e to turbine speed to compressor flow to p_i). However, p_i cannot capture the fast interaction between EVC and AFR , and thus, p_i cannot support a fast feedback loop. The open loop transfer function from EVC to p_i corresponds to a slow real dominant pole:

$$G_{y2} = \frac{1285}{(s + 1.33)[(s + 20)^2 + 0.56]} \quad (11)$$

For fast AFR regulation we rely on a two Degrees of Freedom (2DOF) controller that uses a modification of the cancellation controller (Equation 7), and a slow integrator on p_i :

$$EVC = \frac{0.12}{s} (p_i - p_i^{des}) + C_{red} W_f \quad (12)$$

where, the dynamic feedforward (FF) from W_f to EVC (C_{red}) is derived by filtering the high frequency (>10 rad/s) content of the cancellation controller. One can try to avoid the dynamic FF (cancellation controller, C_{canc}) altogether and instead use a static FF, namely, the DC gain of the cancellation controller $C_{canc}(0)$. Then tune a fast EVC to p_i feedback (FB) controller. A fast FB will need to cancel the slow EVC to p_i pole which introduces robustness issues [8], but hopefully only in low frequencies! However, it is very difficult to tune the FB so that it provides fast AFR response and low EVC overshoot. Recall, that we need to avoid excessive overshoot on EVC that might cause Tq overshoot or EVC saturation. We conclude that the modified cancellation feedforward with the slow integral controller achieve satisfactory response. The linear response of the p_i -based EVC controller is shown in Figure 4 in dash-dot line. Note also that in the case of an unthrottled gasoline (SI or DI) engine cycle-resolved p_i is not meaningful for feedback because it is constant and equal to the atmospheric pressure. In the gasoline engine a UEGO or an EGO sensor can provide the appropriate measurement for AFR feedback control. In this case one should choose the controller Eq. (8)-(10).

We next compare the nonlinear full order AFR response during fueling step changes with equivalent torque step changes for the CIDI engine with the conventional EVC ($EVC=395$) and the controlled EVC . Improvements in the transient response are demonstrated in the linear reduced order model and the nonlinear full order model as shown Figure 6. Similarly with Figure 4, the solid line shows the closed loop response with the controller structure shown in Figure 3 given by Eq. (6)-(7). The dashed line corresponds to the AFR-based controller shown also in Figure 5 given by Eq. (8)-(10). The long-dashed line corresponds to the dash-dot of Figure 4 with the pressure-based

controller given by Eq. (8) and (12). The nonlinear plot includes also the crank-angle resolved cylinder burned gas fraction (F_{cyl}) sampled every cycle when the intake valve closes. F_{cyl} remains always greater than 5% during a transition from the steady state values of 14% to 9%.

5. Conclusions

We demonstrate using simulations that Exhaust Valve Closing (EVC) can be used for management of internal Exhaust Gas Recirculation (iEGR) in turbocharged Diesel engines. Using a combination of static and dynamic feedforward augmented with simple proportional integral controllers we achieve fast regulation of in-cylinder Air-to-Fuel Ratio (AFR) in an effort to reduce visible smoke during torque accelerations. The difficulty in the control tuning arises mostly from the fact that EVC affects both AFR and torque (T_q). Coordination of fueling (W_f) and EVC is, thus required. We show here the methodology for achieving the desired coordination given AFR or intake manifold pressure sensor. It is anticipated that our result can be also used for iEGR and AFR control of unthrottled engines equipped with Variable Valve Timing actuators or for Homogeneous Charge Compression Ignition (HCCI) engines.

6. References:

1. Edwards S. P., Frankle G. R., Wirbeleit F., Raab A., "The Potential of a Combined Miller Cycle and Internal EGR Engine for Future

Heavy Duty Truck Applications," SAE paper 980180.

2. Dekker H., W. Sturm W., "Simulation and Control of a HD Diesel Engine Equipped with new EGR technology," SAE paper 960871.

3. Guzzella L., and Amstutz A., "Control of diesel engines," IEEE Control Systems Magazine, vol.18, No. 2, pp.53-71,1998.

4. Heywood, J.B., *Internal Combustion Engine Fundamentals*," McGraw-Hill, Inc., 1988.

5. Kao, M., and Moskwa, J.J., "Turbocharged diesel engine modeling for nonlinear engine control and estimation," ASME Journal of Dynamic Systems, Measurement and Control, Vol.117, 1995.

6. Moklegaard L., Druzhinina M., Stefanopoulou A., "Compression Braking for Longitudinal Control of Commercial Heavy Vehicles," PATH Report UCB-ITS-PRR-2001-11, April 2001.

7. Najt P., Foster D., "Compression-Ignited Homogeneous Charge Combustion," SAE paper 830264.

8. Skogestad S. and Postlethwaite I., *Multivariable Feedback Control: Analysis, Design*, Wiley, 1996.

9. Stefanopoulou A., Kolmanovsky I.V., and Freudenberg J.S., "Control of Variable Geometry Turbocharged Diesel Engines for Reduced Emissions", IEEE Transactions on Control System Technology, vol.8, No 4, July 2000.

10. Thring R. H., "Homogeneous-Charge Compression-Ignition (HCCI) Engines," SAE paper 892068.

11. Watson, N., and Janota, M.S., "Turbocharging the Internal Combustion Engine," Wiley Interscience, New York, 1982.

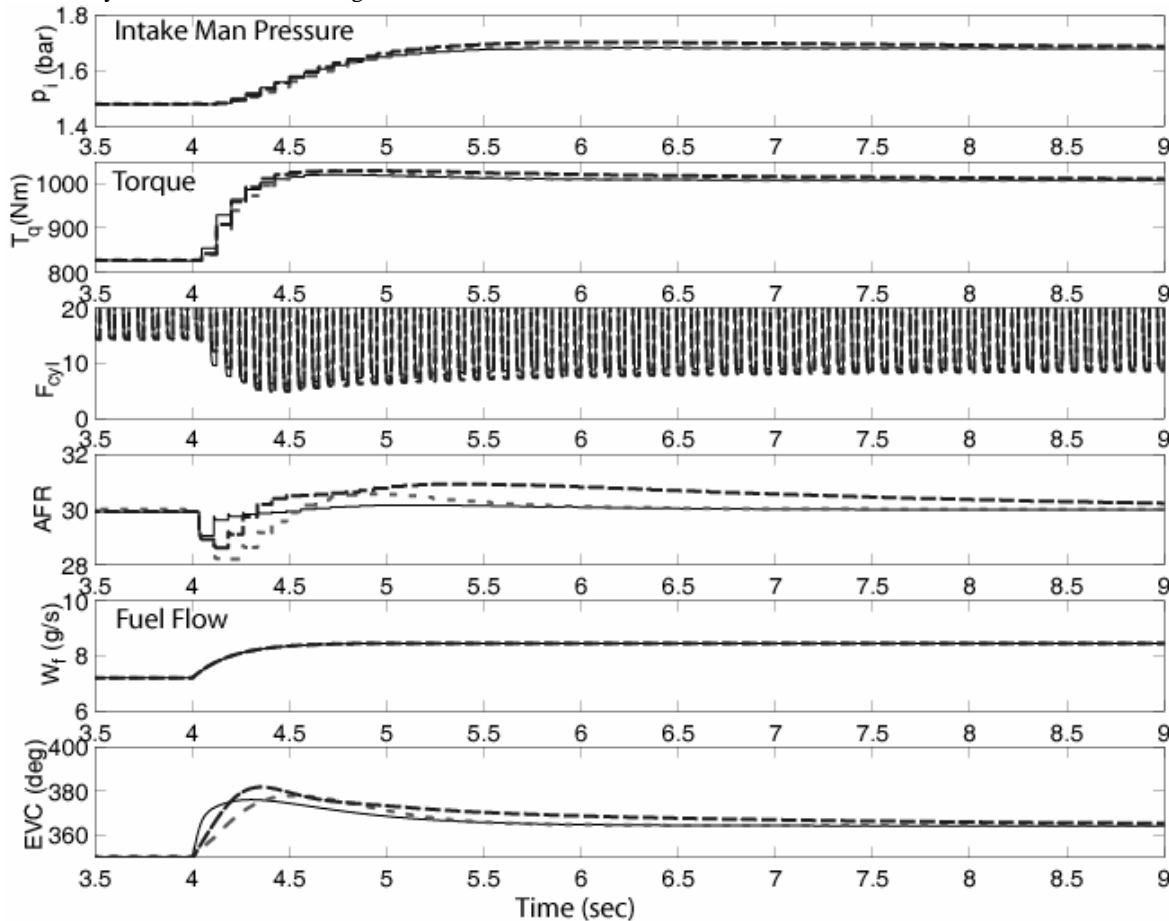


Figure 6. Nonlinear Full Order System Response